

Synthesis, structural and optical characterization of $\text{TeO}_2\text{--GeO}_2\text{--Nd}_2\text{O}_3$ glasses

I. Piroeva¹, L. Dimova^{2*}, S. Atanasova-Vladimirova¹,
N. Petrova², B. L. Shivachev²

¹ Academician Rostislav Kaishev Institute of Physical Chemistry, Bulgarian Academy of Sciences,
Acad. Georgi Bonchev str., building 11, Sofia 1113, Bulgaria

² Academician Ivan Kostov Institute of Mineralogy and Crystallography, Bulgarian Academy of Sciences,
Acad. Georgi Bonchev str., building 107, 1113 Sofia, Bulgaria

Received February, 2013; Revised May, 2013

Synthesis and optical properties of novel $\text{TeO}_2\text{--GeO}_2\text{--Nd}_2\text{O}_3$ glasses suitable for multiband calibration or multicolor filters in the 350–1000 nm wavelength region are reported. Differential thermal analysis (DTA), X-ray diffraction (XRD), Infrared FT-IR, UV/VIS spectroscopy, scanning and transmission electron microscopy (SEM, TEM) were complementarily applied to study the structural, thermal and optical properties of this ternary system. The UV-VIS spectrum shows outstanding absorption at specific wavelength suggesting that the glasses can be employed as multi-color-type filter.

Key words: tellurite glasses, multiband filter, XRD, FTIR.

INTRODUCTION

Tellurium oxide (TeO_2)-based glasses are of scientific and technical interest due to their optical properties: excellent transmission in the visible and near IR (up to 4.5 μm), low phonon energy, large third-order nonlinear susceptibility [1, 2]. In addition to their suitable optical properties tellurite glasses show other favorable properties, such as good mechanical strength and chemical durability, low processing temperature and large rare-earth solubility [3]. The combination of these properties makes tellurite glasses good candidates for the development of optical, nonlinear optical devices (e.g. optical amplifiers) [4]. Multi-band filters are relatively new to the commercial market and are significantly more expensive than traditional colored, dichroic, sequential or polarized filter/glasses [5]. Traditional optics for multiband applications covering regions of the SWIR, MWIR and LWIR include Zinc Sulfide (ZnS), Zinc Selenide (ZnSe) and Germanium (Ge) [6]. These materials have low strength, exhibit very low resistance to water, rain and dust erosion and

ZnS and ZnSe are very soft and easily scratched or damaged. Ge, on the other hand, does not transmit in SWIR and becomes opaque in MWIR and LWIR at temperatures above 100 °C. Current multiband imaging systems with wide field of view use separate cameras and optics for each band region [6]. Achromats can be designed using materials having different dispersion profiles to minimize the focal shift between light from different wavebands when imaged through the lens system [7]. These achromats are currently available only in a narrow wavelength range due to the limited availability of suitable commercial materials.

The aim of this study was to obtain new tellurite glasses possessing suitable mechanical and optical properties for optical application [8]. As a result we report the synthesis, structural and optical properties of $\text{TeO}_2\text{--GeO}_2\text{--Nd}_2\text{O}_3$ glasses that exhibit suitable properties for multiband filter application.

MATERIALS AND METHODS

Synthesis

The tellurite glasses presented in our work were prepared by the melt-quenching technique in platinum crucible in an electrically-heated furnace under ambient atmosphere. High purity chemicals TeO_2

* To whom all correspondence should be sent:
E-mail: louiza.dimova@gmail.com

(99%), GeO₂ (99%), Nd₂O₃ (99%) were used for the batch melting. The raw material batches with composition (1-x)TeO₂-xGeO₂-xNd₂O₃ mol% (x = 5, 10 and 20) were carefully mixed (grounded) and then the batches were melted at 955 °C for 1 h. The glass melts were cast onto a preheated stainless steel mold at 120 °C and annealed at 150 °C (below the glass transition temperature) for 12 h in a separate electric oven to remove thermal strains. Then cooling down to room temperature was performed by switching off the oven. After the annealing the samples were sliced and polished into sizes of 3×3×1 mm³ for the spectroscopic (UV-Vis) measurements.

Differential thermal analysis (DTA)

The DTA curves in the 20–750 °C temperature range were obtained from grounded samples (sample weight 14 ± 0.2 mg) of the as-quenched pieces under a constant heating rate of 10 °C/min in an air flow of 40 ml/min on a Stanton Redcroft thermo-analyzer. The glass transition (*T_g*) and crystallization (*T_c*) temperatures derived from these studies were employed in fixing the annealing-treatment temperatures for the various glass compositions.

X-ray diffraction (XRD)

X-ray powder diffraction analyses (Bruker, D2 Phaser diffractometer, Cu Kα, 0.02°·s⁻¹) were performed on the crushed powders of the annealed and heat-treated samples to verify the amorphous state of the sample and obtain information for the crystalline phases.

Infrared FT-IR

Infrared transmission properties of samples (KBr pellets) were measured with a Bruker Tensor 37 Fourier transform infrared (FTIR) spectrometer at a resolution of 4 cm⁻¹ and accumulating 64 scans.

UV/VIS spectroscopy

The absorption spectra were measured on a Cary100, Varian spectrophotometer over the spectral range of 190–900 nm.

Scanning and transmission electron microscopy (SEM, TEM)

SEM analyses were performed on a JSM 6390 electron microscope (Japan) in conjunction with energy dispersive X-ray spectroscopy (EDS, Oxford INCA Energy 350) equipped with ultrahigh resolution scanning system (ASID-3D) in regimes of secondary electron image (SEI) and back scattered

electrons (BEC) image. Before attempting SEM characterization, the sample must be clean and completely dry. Surface oils or dirt must be removed with solvents such as methanol or acetone. The sample is mounted on a double coated conductive carbon tape that holds the sample firmly to the stage surface and can be used as a ground strap from the sample surface to sample holder. The samples were Carbon coated (time of coating ~20 sec). Carbon at that thickness will have little or no effect on elemental analysis. The accelerating voltage was 20 kV, I ~65 mA. The pressure was of the order of 10⁻⁴ Pa.

TEM work was performed on a JEOL JEM 100B (100 kV). The accelerating voltage was 100 kV and the pressure was of the order of 10⁻⁶ Pa. The preparation of TEM specimens involves mechanical grinding, then dispersion in ethanol and finally depositing a drop of the dispersion on a Cu grid. The grid is dried on a filter paper and is ready for TEM observation.

RESULTS AND DISCUSSION

The XRD patterns of the annealed glasses samples corresponding to the TGN compositions x = 5, 10, and 20 mol% are shown on Fig. 1. The XRD patterns show the amorphous nature of the samples, with some broadening around 2θ = 28° are observed. In order to check for the presence/appearance of metastable phases TEM investigations were also performed to further complement XRD structural characterization. Low magnification TEM images of show the general morphology while the

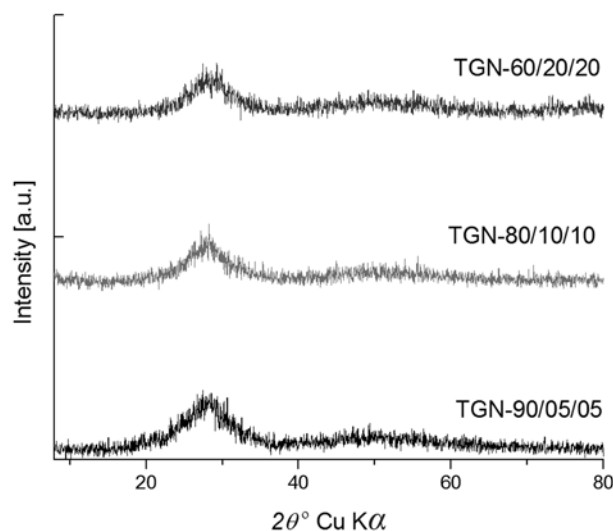


Fig. 1. XRD patterns of TGN-5, TGN-10 and TGN-20 samples after 12 h annealing at 150 °C

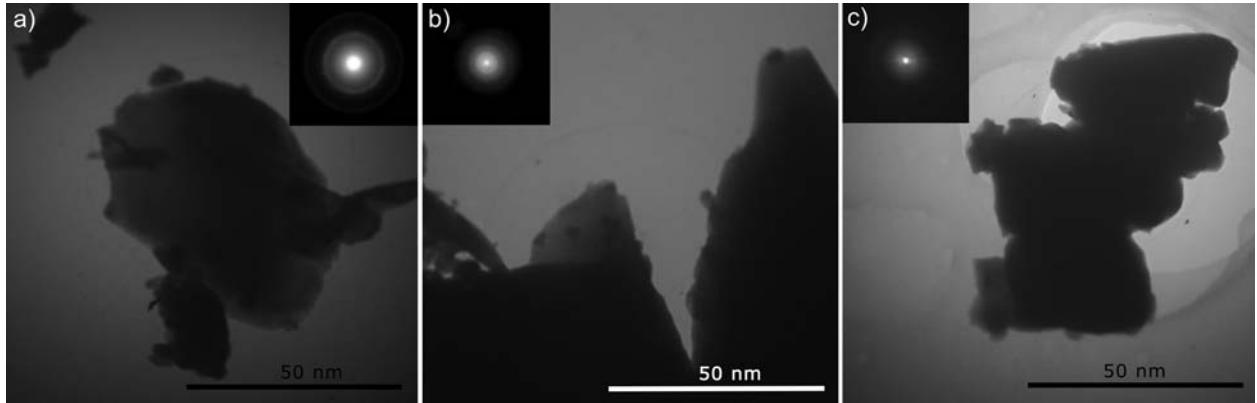


Fig. 2. Selected TEM images and SAED pattern demonstrating the amorphous nature of the samples; a) TGN-5, b) TGN-10 and c) TGN-20

SAED micro diffraction (Fig. 2) shows that samples are amorphous and are not subject to crystallization resulting from the interaction (heating) with the electron beam [9, 10]. The observed halo around the bright spot in the center indicates that the electrons are diffracted randomly by a material of amorphous structure. Indeed DTA data (Fig. 3) shows a good thermal stability of the glasses as the transition temperature (T_g) for all sample is around 320 °C and the first crystallization occurs around 420 °C (for TGN-5). The XRD patterns of the annealed TGN-5 at 300 and 610 °C (Fig. 4) confirm the suggested good thermal stability of the glasses [11]. The annealed at 300 °C (~12h) TGN-5 remains amorphous

while the result of the annealing at 610 °C is the formation of the halite type (NaCl) cubic (SG 225) $\text{Nd}_{0.25}\text{Te}_{0.75}\text{O}_{1.875}$ crystal phase [12].

The compositions of the tellurite glasses and their surface morphology were assessed by SEM/EDS. As one can see the untreated surfaces of the samples exhibit very few visible defects (Fig. 5) and thus are very well suited for optical application (after cutting and polishing). Their chemical compositions were also close to the ones of the starting batches the major difference being for Nd_2O_3 in TGN-20.

The amorphous natures of the synthesized glasses can also be assessed from FTIR analysis [13]. The peaks of the FTIR spectra are very few and large

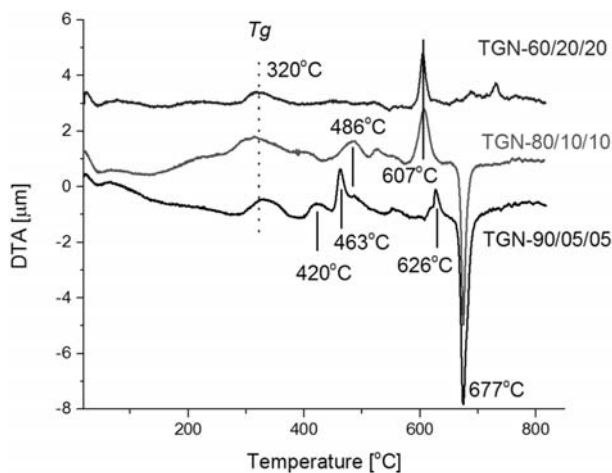


Fig. 3. Differential thermal analysis data of TGN-5, TGN-10 and TGN-20 glass samples

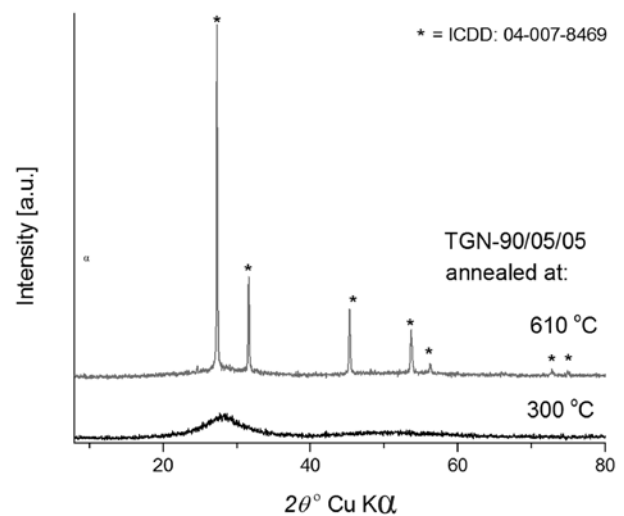


Fig. 4. XRD pattern of TGN-5 after annealing at 300 and 610 °C for 12 hours; JCPDS 04-007-8469 [12]

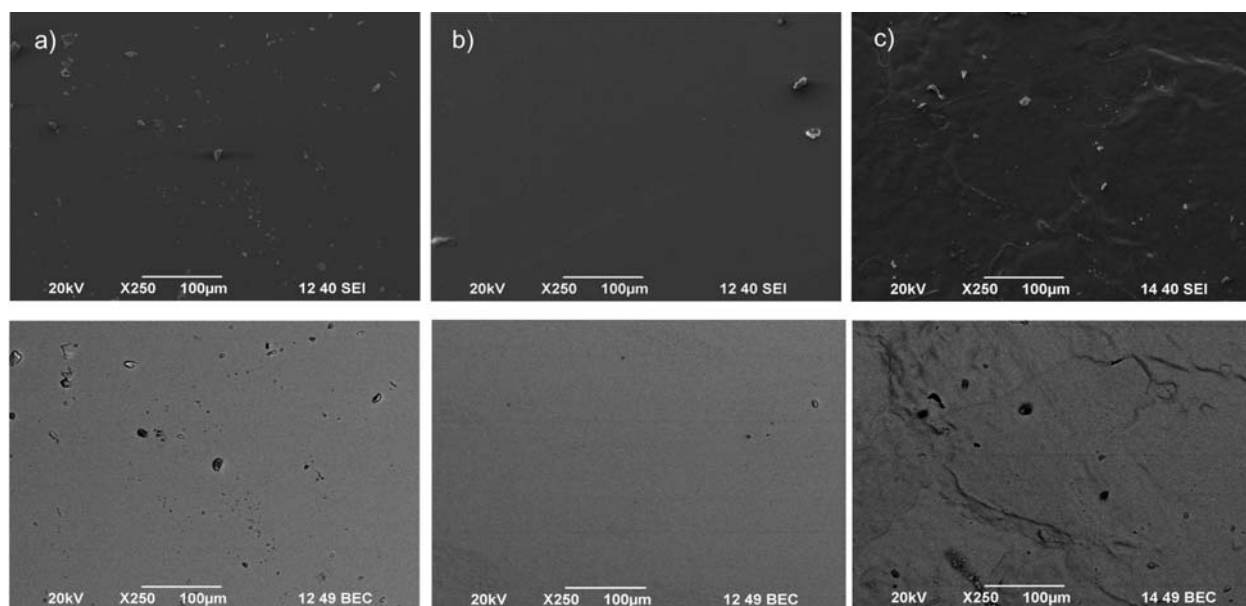


Fig. 5. SEM images of (a) TGN-5, (b) TGN-10 and (c) TGN-20 surfaces. The top row shows images obtained by secondary electron imaging (SEI) while the bottom row are by Backscattered Electron contrast (BEC) imaging

Table 1. Starting chemical composition for TGN – x (x = 5, 10 and 20) mol% samples and subsequent EDS data for obtained samples TGN – x

Starting batch composition (mol%)	EDS data for obtained samples (mol%)	Resulting formula
90/05/05	88.92 / 6.52 / 4.54	88.92 TeO ₂ -6.52GeO ₂ -4.54Nd ₂ O ₃
80/10/10	81.54 / 9.77 / 8.67	81.54 TeO ₂ -9.77GeO ₂ -8.67 Nd ₂ O ₃
60/20/20	63.51 / 19.61 / 16.88	63.51 TeO ₂ -19.61GeO ₂ -16.88 Nd ₂ O ₃

(broad) and thus they reveal only the presence of short order of Te, Ge and Nd oxides (a broad band around 670 cm⁻¹ with a shoulder around 770 cm⁻¹ Fig. 6a). This range is usually associated with stretching vibrations of the Te–O bond: [TeO₄] trigonal bipyramids and [TeO₃] trigonal pyramids units [14]. The performed deconvolution of these bands yield the same results for sample TGN-5 and 10 (90/05/05 and 80/10/10): four peaks with very close values for the peaks maxima. The deconvolution of the FTIR broad band of TGN-20 sample produced seven peaks. Four of those (2, 4, 5 and 6) having approximately the same maxima as the ones in TGN-5 and 10 samples (Fig. 6 b-d). The new peaks are not very intensive and appear on both sides of the broad band at 670–770 cm⁻¹: 471 cm⁻¹, 613 cm⁻¹ and at 900 cm⁻¹. In our case, the absorption band at ~769, 781, 720 cm⁻¹ correlates with [TeO₃] and the one

at ~658, 672, 655 cm⁻¹ with [TeO₄] units [14, 15]. The band located around ~580 cm⁻¹ (584, 587 and 578) can be associated with Te–O–M (M = Nd or Ge) while the band at 828, 845 and 829 cm⁻¹ in the different composition may linked to M–O–M (M = Nd or Ge). The increased amounts of and Nd₂O₃ and GeO₂ lead to additional separation of the M–O–M linkages as Te–O–Ge ones are characterized by the 471 cm⁻¹ band while the 613 cm⁻¹ and 900 cm⁻¹ ones can be attributed to Te–O–Nd and Nd–O–Nd. Those additional bands are could be obtained only in the deconvolution of the TGN-20 spectrum and attempts to introduce them in TGN-5 and TGN-10 processing failed.

The UV-Vis absorbance spectra of the TGN-x samples are shown on Fig. 7. The observed minima of the absorbance are located approximately at 885, 845, 780, 710 (700–725 range), 653 (667–647

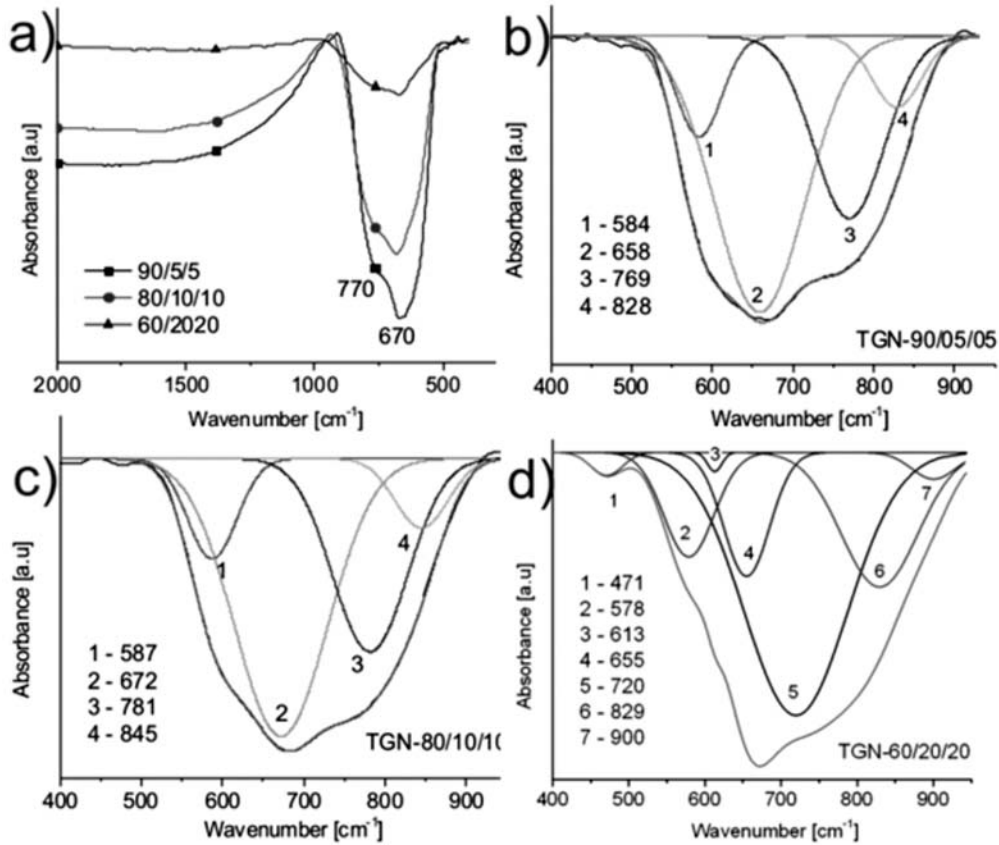


Fig. 6. FTIR spectra of $\text{TeO}_2\text{-GeO}_2\text{-Nd}_2\text{O}_3$ glass: a) Overview of the FTIR of the three TGN – x ($x = 5, 10$ and 20) samples and deconvolution of the band around 760 cm^{-1} for each sample b) TGN – 5, c) TGN – 10 and d) TGN – 20

range), 547, 491 and 447 nm [16]. The maxima of the absorption correspond to Nd^{3+} transitions from ground state of $^4\text{I}_{9/2}$ to the excited state of

$^4\text{F}_{3/2}$ (876 nm), $^4\text{F}_{5/2}$ (804 nm), $^4\text{F}_{7/2}$ (747 nm), $^4\text{F}_{9/2}$ (682 nm), $^2\text{H}_{11/2}$ (628 nm), $^4\text{G}_{5/2}$ (583 nm), $^4\text{G}_{7/2}$ (525 nm), $^4\text{G}_{9/2}$ (511 nm), $^4\text{G}_{11/2}$ (465 nm) and $^2\text{P}_{1/2}$ (431 nm) respectively. The most interesting feature of the obtained glasses is probably their UV-Vis optical characteristics showing that they can be used as multiband filters.

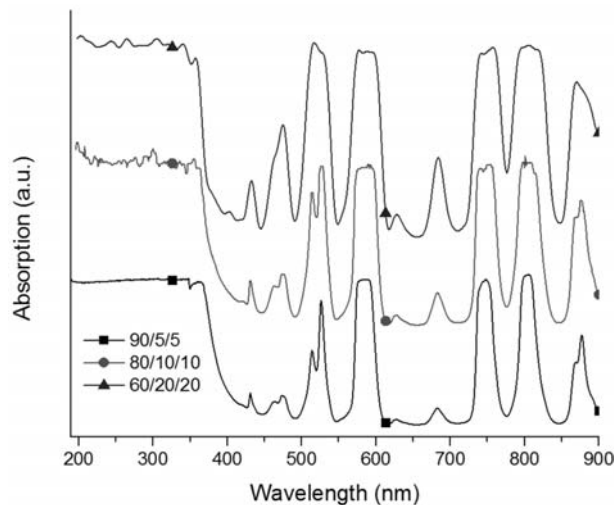


Fig. 7. UV-Visible transmittance spectra of polished 1 mm thick $\text{TeO}_2\text{-GeO}_2\text{-Nd}_2\text{O}_3$ glasses

CONCLUSIONS

In summary we have prepared $\text{TeO}_2\text{-GeO}_2\text{-Nd}_2\text{O}_3$ glasses by conventional melt-quenching technique. The glasses show good thermal stability, with respect to other tellurite glasses, which makes them suitable for usage up to $\sim 250\text{ }^\circ\text{C}$. The optical absorbance/transmission properties of the glasses are comparable to those of the multiband filters and make them ready for this type of application.

Acknowledgments: The authors would like to thank the Bulgarian National Science Fund (bulfund.com) support through grant DRNF 02/1.

REFERENCES

1. R. El-Mallawany, *Tellurite Glasses Handbook: Physical Properties and Data*, 2-nd ed. CRC Press, Proc. conf., Bordeaux, France, 2011.
2. A. Bachvarova-Nedelcheva, R. Iordanova, K. L. Kostov, St. Yordanov, V. Ganev, *Optical Mater.*, **34**, 1781 (2012).
3. G. Yankov, L. Dimowa, N. Petrova, M. Tarassov, K. Dimitrov, T. Petrov, B. L. Shivachev, *Optical Mater.*, **35**, 248 (2012).
4. H. Hu, Y. Bai, M. Huang, B. Qin, J. Liu, W. Zheng, *Optical Mater.*, **34**, 274 (2011).
5. H. T. Bookey, J. Lousteau, A. Jha, N. Gayraud, R. R. Thomson, N. D. Psaila, H. Li, W. N. MacPherson, J. S. Barton, A. K. Kar., *Optics Express*, **15**, 17554 (2007).
6. I. Jlassi, H. Elhouichet, M. Ferid, C. Barthou, *J. Lumi.*, **130**, 2394 (2010).
7. S. Bayya, J. Sanghera, W. Kim, G. Villalobos, I. Aggarwal, *Optical Components and Materials*, IX, 825703 (2012); doi:10.1117/12.910149.
8. Y. Dimitriev, A. Bachvarova-Nedelcheva, R. Iordanova, S. Yordanov, *Phys. Chem. Glasses*, B, **48**, 138 (2007).
9. B. Fultz, J. Howe, *Transmission Electron Microscopy and Diffractometry of Materials*, 3-rd edition, Springer, 2007.
10. P. Binev, W. Dahmen, R. DeVore, P. Lamby, D. I. Savu, R. Sharpley, *Nanostructure Science and Technology*, **73** (2012).
11. Z. Luo, A. Lu, G. Qu, Y. Lei, *Journal of Non-Crystalline Solids*, **362**, 1, 207 (2013).
12. M. Tromel, W. Hutzler, E. Munch, *J. Less-Common Met.*, **110**, 421 (1985).
13. Y. Dimitriev, V. Dimitrov, M. Arnaudov, *Journal of Materials Science*, **18**, 5 1353 (1983).
14. E. I. Kamitsos, A. Patsis, M. Karakassides, G. Chrysikos, *Journal of Non-Crystalline Solids*, **126**, 1–2, 52 (1990).
15. Q. Li, L. Tian, K. Chi, H. Yang, M. Sun, W. Fu, *Applied Surface Science*, **270**, 707 (2013).
16. G. Singh, P. Kaur, S. Kaur, D. Arora, P. Singh, D. Sing, *Materials Physics and Mechanics*, **14**, 31 (2012).

СИНТЕЗ, СТРУКТУРНА И ОПТИЧНА ХАРАКТЕРИСТИКА НА $\text{TeO}_2\text{-GeO}_2\text{-Nd}_2\text{O}_3$ СЪКЛА

И. Пироева², Л. Димова¹, С. Атанасова-Владиминова²,
Н. Петрова¹, Б. Шивачев¹

¹ *Институт по минералогия и кристалография, БАН, ул. „Акад. Георги Бончев“, бл. 107, София 1113, България*

² *Институт по физикохимия „Акад. Ростислав Каишев“, БАН, ул. „Акад. Георги Бончев“, бл. 11, София 1113, България*

Постъпила февруари, 2013 г.; приета май, 2013 г.

(Резюме)

В настоящата работа са представени синтезът, структурните, термичните и оптичните особености на нови съкла от системата $\text{TeO}_2\text{-GeO}_2\text{-Nd}_2\text{O}_3$. Получените съкла могат да намерят приложение като цветни филтри при калибриране, изискващо наличие на няколко дължини на вълните в диапазона 350–1000 nm и т.н. При охарактеризирането на съклата са използвани диференциално термичен анализ (ДТА), прахова рентгенова дифракция (ПРД), инфрачервена спектроскопия (ИР), ултравиолетова и видима абсорбция (УВ-Вис) и електронна микроскопия (сканираща и трансмисионна). УВ-Вис спектърът на поглъщане на изследваните образци показва специфично поглъщане на определени дължини на вълната.